Honda Research Institute EU
Honda Research Institute Europe GmbH
https://www.honda-ri.de/

Hybrid Strategy Coupling EGO and CMA-ES for the Topology Optimization of Crash Structures

Elena Raponi, Mariusz Bujny, Markus Olhofer, Simonetta Boria, Fabian Duddeck

2021

Preprint:

This is a post-peer-review, pre-copyedit version of an article published in Computational Intelligence. IJCCI 2019.. The final authenticated version is available online at: https://doi.org/10.1007/978-3-030-70594-7_3

Hybrid Strategy Coupling EGO and CMA-ES for Structural Topology Optimization in Statics and Crashworthiness

Elena Raponi, Mariusz Bujny, Markus Olhofer, Simonetta Boria, and Fabian Duddeck

Abstract Topology Optimization (TO) represents a relevant tool in the design of mechanical structures and, as such, it is currently used in many industrial applications. However, many TO optimization techniques are still questionable when applied to crashworthiness optimization problems due to their complexity and lack of gradient information. The aim of this work is to describe the Hybrid Kriging-assisted Level Set Method (HKG-LSM) and test its performance in the optimization of mechanical structures consisting of ensembles of beams subjected to both static and dynamic loads. The algorithm adopts a low-dimensional parametrization introduced by the Evolutionary Level Set Method (EA-LSM) for structural Topology Optimization and couples the Efficient Global Optimization (EGO) and the Covariance Matrix Adaptation Evolution Strategy (CMA-ES) to converge towards the optimum within a fixed budget of evaluations. It takes advantage of the explorative capabilities of EGO ensuring a fast convergence at the beginning of the optimization procedure, as well as the flexibility and robustness of CMA-ES to exploit promising regions of the search space Precisely, HKG-LSM first uses the Kriging-based method for Level Set Topology Optimization (KG-LSM) and afterwards switches to the EA-LSM using CMA-ES, whose parameters are initialized based on the previous model. Within the research, a minimum compliance cantilever beam test case is used to validate the presented strategy at different dimensionalities, up to 15 variables. The method is then applied to a 15-variables 2D crash test case, consisting of a cylindrical pole impact on a rectangular beam fixed at both ends. Results show that HKG-LSM performs well in terms of convergence speed and hence represents a valuable option in real-world applications with limited computational resources.

E. Raponi (✉) · S. Boria
School of Sciences and Technology, Department of Mathematics, University of Camerino, Camerino, Italy
e-mail: elena.raponi@unicam.it

M. Bujny · M. Olhofer
Honda Research Institute Europe GmbH, Offenbach am Main, Germany

F. Duddeck
Department of Civil, Geo and Environmental Engineering, Technical University of Munich, Munich, Germany

© Springer Nature Switzerland AG 2021

J. J. Merelo et al. (eds.), *Computational Intelligence*, Studies in Computational Intelligence 922, https://doi.org/10.1007/978-3-030-70594-7_3

Keywords Topology optimization · Crashworthiness optimization · Hybrid methods · Surrogate modeling · Kriging · Evolution strategies · Level set method · Moving morphable components

1 Introduction

Vehicle safety is one of the most studied research areas in automotive engineering over recent decades. In order to test mechanical components, many physical experiments are needed. These are characterized by prohibitive times and costs, and hence particular attention has to be paid to the design phase of structures. Computer-Aided Design (CAD) methods and numerical simulations with the Finite Element Method (FEM) have become a standard for the design and analysis of mechanical structures, leading to a rapid development of Structural Topology Optimization (TO) [5]. TO is a well-developed discipline that aims to generate optimal component structures through changing material distribution in a given design space under defined boundary conditions (supports, forces). It is currently applied in many engineering fields, however the most known TO approaches for crashworthiness applications might be questioned. In fact, they use simplifications that frequently do not take into account essential aspects of the crash problem, e.g. nonlinearities, numerical noise, and discontinuities of the objective functions to be optimized. Such approaches can be collected in the following categories: Equivalent Static Loads method [9, 22], Ground Structure Approaches [30], Bubble and Graph/Heuristic-based Approaches [11, 28], Hybrid Cellular Automata methods [10, 27], and State-based representation approaches [3, 4].

In this context, more general optimizers which do not require any gradient or sensitivity information to carry out the optimization procedure deserve special attention. In particular, Evolution Strategies (ESs) (e.g., the Covariance Matrix Adaptation Evolution Strategy (CMA-ES) [18]) and the Efficient Global Optimization (EGO) [13] demonstrated to be valid alternatives.

On the one hand, ESs are optimization techniques based on the iterative creation of generations of individuals, corresponding to different points of the search space, which only need the direct evaluation of the objective function to move forward towards the optimum. Compared to other global optimization techniques, these algorithms are easy to implement and very often provide adequate solutions, showing many advantages such as simplicity, robust responses to changing circumstances and flexibility. However, they normally require thousands of calls to the high-fidelity analysis codes to locate a near optimal solution, leading to very high numerical costs, which are proportional to the problem dimensionality.

On the other hand, EGO allows for replacing the direct optimization of the computationally expensive model by an iterative process composed of the creation, optimization and update of a model approximating the original function, referred to as surrogate model. This model is much cheaper to run and can be used to perform many more evaluations during the optimization process. Starting from a limited set

of points defined in the problem domain and the evaluation of the objective function on such a set, a first approximation is constructed. Afterwards, new promising points are selected and the model is updated according to them. Nonetheless, surrogate-based optimization shows some limitation with the increasing of dimensionality and iterations of the algorithm, turning out to have poorer exploitive capabilities than ESs [33].

One attempt to combine the positive aspects of EGO and CMA-ES at different stages of the optimization process was made by Raponi et al. [34], who proposed the Hybrid Kriging-assisted Level Set Method (HKG-LSM) for Structural Topology Optimization. This strategy is composed of three major building blocks:

- Level Set Method (LSM) [1, 15, 29], which defines the material distribution changes based on a low-dimensional implicit parametrization of the material boundaries by means of local Level Set Functions (LSFs), also referred to as Movable Morphable Components (MMCs) [14];
- Kriging-guided Level Set Method (KG-LSM) [32, 33], which constructs a cheap approximating model according to an initial set of training points. Based on the data points and the committed error in the approximation, it updates the model iteratively and allows for obtaining a trade-off between exploration and exploitation of the domain space, which results in a fast convergence of the algorithm towards promising areas;
- Evolutionary Level Set Method (EA-LSM) for crash Topology Optimization [6, 7], embedding CMA-ES, to which the proposed optimization algorithm switches when no improvement on the optimal design is found within a prescribed number of evaluations. Its main role is to investigate the detected good region and further exploit it in order to locally optimize the current design.

This research is an extension of the aforementioned work [33], aiming to validate the HKG-LSM algorithm in optimization problems characterized by a higher dimensionality. Moreover, it applies the algorithm to a crashworthiness scenario for the first time. More precisely, HKG-LSM is here evaluated on a static cantilever beam, as well as on a dynamic pole intrusion test case for a fixed budget of FEM evaluations. This choice is dictated by the fact that in many industrial applications, FEM evaluations are very expensive and, as such, limited.

The paper is structured as follows. Section 2 describes the implicit parametrization used to represent the problem and the geometry mapping to the mechanical model. In Sect. 3, the addressed optimization problem is defined, together with its constraints, which are necessary in order to produce physically consistent and well-performing structures. In Sect. 4, the resolution strategy consisting of the combination of KG-LSM with EA-LSM is presented. Section 5 illustrates the static and dynamic test cases used to evaluate the proposed approach, while the experimental campaign and its results are discussed in Sects. 6 and 7, respectively. Conclusions are drawn at the end in Sect. 8.

2 Problem Representation

The HKG-LSM is designed for to of crash structures. Therefore, it is aimed at easily handling the unpredictability, noisiness, discontinuities and lack of gradient information which characterize the crashworthiness design optimization problems. Since in structural mechanics optimal topologies frequently consist of ensembles of interconnected beams, on the basis of previous studies [7, 14, 33], the mechanical structure consists of a set of MMCS whose boundaries are implicitly defined by iso-contours of an LSF.

2.1 Parametrization

The proposed parametrization was introduced in previous works [7, 33]. It is based on a global LSF Φ defined as:

$$\begin{cases} \Phi(\mathbf{u}) > 0, & \mathbf{u} \in \Omega, \\ \Phi(\mathbf{u}) = 0, & \mathbf{u} \in \partial\Omega, \\ \Phi(\mathbf{u}) < 0, & \mathbf{u} \in D \backslash \Omega. \end{cases} \tag{1}$$

Here, Ω denotes the region of the domain D occupied by material, while $D\backslash\Omega$ is the complementary set, occupied by void. The interface between material and void is given by $\partial\Omega$. Hence, in this approach intermediate densities do not occur for each $\mathbf{u} = (x, y)^T \in D$.

A representation of this global LSF for complex geometries is difficult; therefore, it is constructed by a set of local LSFs given by:

$$\begin{cases} \phi_i(\mathbf{u}) > 0, & \mathbf{u} \in \Omega_i, \\ \phi_i(\mathbf{u}) = 0, & \mathbf{u} \in \partial\Omega_i, \\ \phi_i(\mathbf{u}) < 0, & \mathbf{u} \in D \backslash \Omega_i, \end{cases} \tag{2}$$

where ϕ_i is the local LSF of the ith component occupying the design domain subregion Ω_i.

The total region of the domain D is hence constructed by the union of e elementary components:

$$\Omega = \bigcup_{i=1}^{e} \Omega_i. \tag{3}$$

To reduce the number of parameters, we propose inspired by Guo et al. [14] to use beams as local basis functions having the mathematical form:

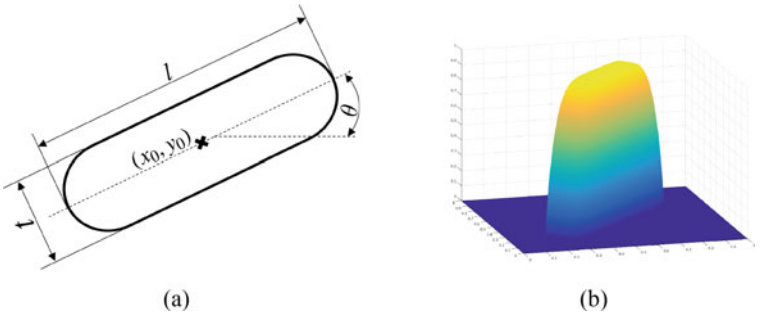


Fig. 1 Structural component details [7]: **a** component parametrization, **b** corresponding local LSF, where negative values are set to zero [33]

$$\phi_i(\mathbf{u}) = -\left[\left(\frac{\cos\theta_i\,(x - x_{0i}) + \sin\theta_i\,\left(y - y_{0i}\right)}{l_i/2}\right)^m + \left(\frac{-\sin\theta_i\,(x - x_{0i}) + \cos\theta_i\,\left(y - y_{0i}\right)}{t_i/2}\right)^m - 1\right], \tag{4}$$

where $\mathbf{u} = (x, y)^T$ is a point of the bi-dimensional domain $D = \mathbb{R}^2$ and (x_0, y_0) denotes the position of the center of the component with length l and thickness t; in addition, the beam component is oriented inside the domain by the rotation angle θ, see Fig. 1a. The integer m is a method parameter to be chosen by the user; it should be even and relatively large. In this study, $m = 6$ is used. The variation of the local LSF parameters enables to move, shrink, dilate, and rotate a single beam component. Figure 1b depicts a 3-dimensional plot of the ith local LSF corresponding to the definition given in Eq. (4).

2.2 Geometry Mapping

For Level Set Topology Optimization it is essential to choose an appropriate mapping from the geometry representation defined by the LSF to the mechanical, i.e. computational model. Here, motivated by its simplicity, a density-based geometry mapping is used:

$$\mathbf{E}(\mathbf{u}) = \rho(\mathbf{u})\,\mathbf{E}^0 \qquad 0 \leq \rho(\mathbf{u}) \leq 1, \tag{5}$$

where $\rho(\mathbf{u})$ is the density at the point $\mathbf{u} \in D$ and $\mathbf{E}^0$ is the reference quantity of the elasticity tensor. By this approach, the density $\rho(\mathbf{u})$ at position $\mathbf{u}$ can be obtained from the LSF $\Phi(\mathbf{u})$ via:

$$\rho(\mathbf{u}) = H(\Phi(\mathbf{u}))\,. \tag{6}$$

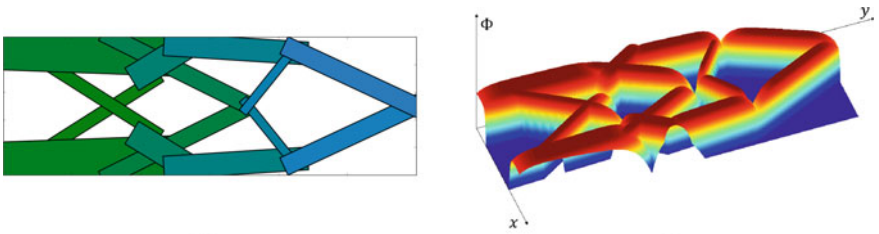


Fig. 2 Combination of local LSFs: **a** illustrative structural layout, **b** plot of the global LSF, where negative values are set to zero [33]

Note, that the global LSF is taken here as the maximum of the local ones at position $\mathbf{u}$:

$$\Phi(\mathbf{u}) = \max(\phi_1(\mathbf{u}), \phi_2(\mathbf{u}), \ldots, \phi_e(\mathbf{u})). \tag{7}$$

Here, $H(x)$ is the Heaviside function, which is defined as:

$$H(x) = \begin{cases} 0, & \text{if } x < 0, \\ 1, & \text{if } x \geq 0. \end{cases} \tag{8}$$

Figure 2 shows an example of the composition of local LSFs, resulting in the global LSF defined by Eq. (7).

3 Optimization Problem and Constraints

In this work, an optimization problem of the following form is considered:

$$\begin{aligned} \min_{\mathbf{x}} \quad & f_{\text{obj}}(\mathbf{x}), \\ \text{s.t.} \quad & \mathbf{KU} = \mathbf{F}/r(t) = 0, \\ & g(\mathbf{x}) \leq 0, \quad \mathbf{x} \in \mathbb{R}^k, \end{aligned} \tag{9}$$

where f_{obj} is the objective function that is minimized, $\mathbf{KU} = \mathbf{F}$ denotes the equilibrium condition for the static test case, $r(t) = 0$ represents the equilibrium condition at time t when a dynamic test case is considered, and g is the inequality constraint. The objective function is evaluated on the vector $\mathbf{x} \in \mathbb{R}^k$ of the design variables, which collects all the parameters defining the LSM basis functions.

In the static test cases, f_{obj} is the compliance (i.e., the inverse of the stiffness) of a cantilever beam, while the pole intrusion was chosen as objective function in the crash scenario. The optimization is carried out while respecting a $g(\mathbf{x}) = V(\mathbf{x}) - V_{\text{req}} \leq 0$ constraint, which requires the volume V of the analyzed structure not to exceed

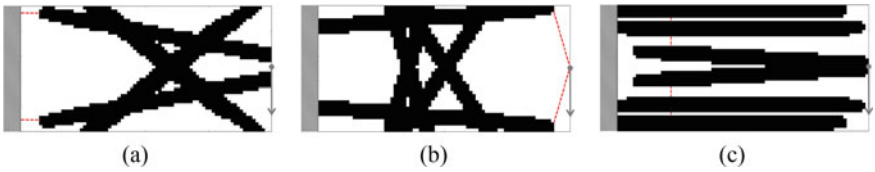


Fig. 3 Violation of the connectivity constraint regarding **a** the connection to the support, **b** the connection to the load, **c** the connection of the structure itself. The distances prohibiting the design to fulfill the connectivity criteria are represented by the dashed lines [33, 34]

a prescribed limit V_{req} equal to 50% of the design domain volume. Throughout the optimization process, disconnected structures can be generated, as illustrated in Fig. 3. Therefore, in order to obtain physically consistent structural layouts, a connectivity constraint is also considered. It ensures that the optimized structures make sense from the physical point of view, while the volume constraint is imposed in order to make the structures fulfill the industrial requirements of limited mass. When the static cantilever beam test case is analyzed, each material distribution is required to be connected to the support on the left-hand side of the domain, to the load that the structure is subjected to on the right-hand side, and has to respect a connection of the structure to itself, i.e. a material path from the support to the load has to be found. Figure 3 shows three material distributions, each representing the violation of the connectivity constraint according to the first, second and third criterion, respectively. On the other hand, in the dynamic pole intrusion test case, the connection to the load is replaced by the connection of the structure to the right-hand side support. According to the phase of the optimization procedure, i.e. the sub-algorithm that is currently used, two different techniques are used to handle such constraints, which are described in Sect. 4.2.

4 Resolution Strategy

In the next part, the principles of the optimization approach proposed in this paper are described. The main idea is to realize a new hybrid strategy for the optimization of structures by combining sequentially the following two steps:

– EGO method with a Kriging Level Set method (KG-LSM) and
– CMA-ES approach incorporated in an Evolutionary Level Set Method (EA-LSM).

This hybridization, named here HKG-LSM, is motivated by the high efficiency of the EGO in the early stage of the optimization for design space exploration via the infill procedures and the superior performance of the CMA-ES for exploitation in the later phase (local search and convergence).

4.1 Optimization Algorithm

The optimization approach proposed here, i.e. the HKG-LSM, is especially adapted to solve efficiently structural design problems. To illustrate the method, it is applied first to linear and static cantilever beam test cases; then, in the final part of this paper, it is used for the optimization of a nonlinear, transient crash case. The first sub-algorithm of the HKG-LSM is based on a redraft of the EGO method taken as proposed by [2, 20], applied to a Kriging surrogate model. Then, the approach switches to the second sub-algorithm, the CMA-ES, to refine the best structure obtained by the first sub-algorithm; an outline of the developed optimization method is provided in Algorithm 1.

Data: initial data set $(\mathbf{X}, \mathbf{Y})$ with n sample points, where $\mathbf{X} = \{\mathbf{x}^{(1)}, \mathbf{x}^{(2)}, \ldots, \mathbf{x}^{(n)}\}^T$
$i := 1$;
while $i < n$ **do**
  check feasibility of point $\mathbf{x}^{(i)}$;
  if $\mathbf{x}^{(i)}$ *infeasible* **then**
    $\mathbf{X} := \mathbf{X} \backslash \{\mathbf{x}^{(i)}\}$
  end
  $i := i + 1$;
end
$y^* := \min(\mathbf{Y})$;
$\mathbf{x}^* := \mathbf{x} \in \mathbf{X} : y(\mathbf{x}) = y^*$;
$t := 0$;
$c := 1$
while $t < n_{\max}$ *and* $c < c_{\max}$ **do**
  fit Kriging to available data $(\mathbf{X}, \mathbf{Y})$;
  find infill point: $\mathbf{p} := \operatorname{argmax}_{\mathbf{x}} \overline{\mathrm{EICD}}(\mathbf{x})$ (Eq. (25));
  update sample set: $\mathbf{X} := \mathbf{X} \cup \mathbf{p}$;
  update response set: $\mathbf{Y} := \mathbf{Y} \cup y(\mathbf{p})$;
  if $\min(\mathbf{Y}) < y^*$ **then**
    $c := 1$;
    $y^* := \min(\mathbf{Y})$;
    $\mathbf{x}^* := \mathbf{x} \in \mathbf{X} : y(\mathbf{x}) = y^*$;
  else
    $c := c + 1$;
  end
  $t := t + 1$;
end
initialize CMA-ES parameters $(\boldsymbol{\sigma}, \boldsymbol{C})$;
initialize parent design: $\mathbf{x} = \mathbf{x}^*$;
run CMA-ES.

Algorithm 1: HKG-LSM optimization algorithm [34]. The reference algorithm for the CMA-ES can be found in the work by Hansen [17].

The procedure starts with the Design of Experiments (DoE) [13] generating samples in the design space and selecting a set of training points to compute the objective function using the high-fidelity model (i.e. finite element model). For this, an Optimal Latin Hypercube Sampling (OHLS) [12] is used, which leads to a training dataset $\mathbf{X} = \{\mathbf{x}^{(1)}, \mathbf{x}^{(2)}, \ldots, \mathbf{x}^{(n)}\}^T$ with the observed responses $\mathbf{y} = \{y^{(1)}, y^{(2)}, \ldots, y^{(n)}\}^T$. Then, the feasibility w.r.t. volume and connectivity constraints is checked for all points and a Kriging surrogate model is constructed and iteratively updated. As soon as the maximum number of iterations without design improvement is reached, the second stage is started, i.e. the overall optimizer progresses from the Kriging-based strategy to the CMA-ES-based approach. The parent design for the latter is set to be the best structure found in the first optimization stage.

4.1.1 Kriging Model

The Kriging surrogate model, for details see e.g. [2, 8, 13, 21], is used to predict values of an unknown response function at a selected new point by computing a weighted average of the already known values of the function in the vicinity of that point. Starting from a set of sample points $\mathbf{X}$ with observed responses $\mathbf{y}$, the value of the objective function at a new location $\mathbf{x}$ is approximated by the value from the surrogate.

For Kriging, the training data is interpreted as results of a stochastic process, which can be described using a set of random vectors of the form $\mathbf{Y}(\mathbf{x}) = (Y(\mathbf{x}^{(1)}), \ldots, Y(\mathbf{x}^{(n)}))^T$ with mean $\mathbf{1}\mu$, where $\mathbf{1}$ is an nx1 column vector of ones. In addition, let the correlation between each couple of random variables be described via a basis function expression:

$$\mathrm{cor}[Y(\mathbf{x}^{(i)}), Y(\mathbf{x}^{(l)})] = \exp\left(-\sum_{j=1}^{k} \theta_j |x_j^{(i)} - x_j^{(l)}|^2\right), \tag{10}$$

where $\boldsymbol{\theta}$ is a vector parameter allowing the width of the basis function to differ from variable to variable. The correlations depend on the absolute distance between the sample points and on the parameters θ_j, which are estimated by using the likelihood of the predicted data $\mathbf{y}$ [13]:

$$L = \frac{1}{(2\pi\sigma^2)^{n/2}|\boldsymbol{\Psi}|^{1/2}} \exp\left(-\frac{(\mathbf{y} - \mathbf{1}\mu)^T \boldsymbol{\Psi}^{-1}(\mathbf{y} - \mathbf{1}\mu)}{2\sigma^2}\right). \tag{11}$$

After appropriate substitutions and simplifications, the natural logarithm of Eq. (11) is considered. By deriving and setting the derivative to zero, the maximum likelihood estimates (MLEs) for the mean μ and variance σ^2 are obtained:

$$\hat{\mu} = \frac{\mathbf{1}^T \boldsymbol{\Psi}^{-1} \mathbf{y}}{\mathbf{1}^T \boldsymbol{\Psi}^{-1} \mathbf{1}}, \quad \hat{\sigma}^2 = \frac{(\mathbf{y} - \mathbf{1}\mu)^T \boldsymbol{\Psi}^{-1}(\mathbf{y} - \mathbf{1}\mu)}{n}, \tag{12}$$

where $\boldsymbol{\Psi}$ is the correlation matrix between the random variables. Finally, the model correlation can be utilized to predict new values based on the observed data. By augmenting the model data with a new input $\mathbf{x}$ and the corresponding output $\hat{y}$ and maximizing the likelihood of the augmented data, the prediction of the response at the new location, the mean value $\hat{y}$, and the committed error in the prediction $\hat{s}^2$ are determined:

$$\hat{y}(\mathbf{x}) = \hat{\mu} + \psi^T \boldsymbol{\Psi}^{-1}(\mathbf{y} - \mathbf{1}\hat{\mu}), \tag{13}$$

$$\hat{s}^2(\mathbf{x}) = \hat{\sigma}^2 \left[1 - \psi^T \boldsymbol{\Psi}^{-1} \psi + \frac{1 - \mathbf{1}^T \boldsymbol{\Psi}^{-1} \psi}{\mathbf{1} \boldsymbol{\Psi}^{-1} \mathbf{1}} \right]. \tag{14}$$

4.1.2 Efficient Global Optimization

After the selection and construction of the surrogate model by fitting it to the initial DoE data, the optimization process starts. Here, compared to any evolutionary algorithm, the advantage of choosing EGO as surrogate technique becomes apparent (especially for non-parallelized processes); each iteration consists of only a single call of the expensive high-fidelity model, the proposed infill point, guiding the search towards the optimum of the optimization problem and providing new high-fidelity data for an update of the surrogate.

Among other techniques for the choice of the locations for the infill points, this work uses a modified version of Expected Improvement (EI) [13], taking into account the connectivity and the volume constraints as described in Sect. 4.2 [33].

Since one goal of the infill search is to position the next point in order to improve the best observed value so far ($y_{\min}$), the EI criterion aims to look for an infill position that maximizes the amount of improvement (defined as $I(\mathbf{x}) = \max(y_{\min} - Y(\mathbf{x}), 0)$) over the value of the objective function measured on the current optimum:

$$\mathbf{x}_{\text{infill}} = \underset{\mathbf{x}}{\operatorname{argmax}} \; E[I(\mathbf{x})]. \tag{15}$$

In turn, the EI is defined as follows:

$$E[I(\mathbf{x})] = \begin{cases} (y_{\min} - \hat{y}(\mathbf{x}))\Phi_Y \left(\dfrac{y_{\min} - \hat{y}(\mathbf{x})}{\hat{s}(\mathbf{x})} \right) & \\ + \hat{s}(\mathbf{x})\phi_Y \left(\dfrac{y_{\min} - \hat{y}(\mathbf{x})}{\hat{s}(\mathbf{x})} \right) & \text{if } \hat{s}(\mathbf{x}) > 0 \\ 0 & \text{if } \hat{s}(\mathbf{x}) = 0 \end{cases} \tag{16}$$

where Φ_Y and ϕ_Y are the Gaussian cumulative distribution function and probability density function, respectively.

Equation (16) can be seen as sum of two terms:

– the first term, proportional to $(y_{\min} - \hat{y}(\mathbf{x}))$, which controls the exploitative tendency of the search criterion;
– the second term, proportional to $\hat{s}(\mathbf{x})$, whose predominance would lead to an explorative choice of the new infill point.

Therefore, the EI infill criterion represents a good trade-off between exploitation and exploration.

4.1.3 Covariance Matrix Adaptation Evolution Strategy

CMA-ES [17] is a popular algorithm for global optimization problems. The (μ, λ)-CMA-ES relies on the iterative sampling and updating of a multivariate normal density

$$\mathbf{x}_k^{(g+1)} \sim \mathbf{N}\left(\langle \mathbf{x} \rangle_w^{(g)}, {\sigma^{(g)}}^2 \mathbf{C}^{(g)}\right), \quad k = 1, \ldots, \lambda \tag{17}$$

where g is the iteration counter, $\sigma^{(g)} \in \mathbb{R}^+$ is the mutation step size, which controls the step length, and $\mathbf{C}^{(g)} \in \mathbb{R}^{n \times n}$, where n is the dimensionality of the problem, is a covariance matrix. CMA-ES is a derandomized Evolution Strategy, which adapts the covariance matrix of the normal distribution on the basis of the previous search steps [19]. Such matrix represents pairwise dependencies between the problem variables and its update during the optimization procedure is of particular importance when dealing with ill-conditioned objective functions.

Regarding Eq. (17), λ is the offspring population size and $\langle x \rangle_w^{(g)}$ is the recombination point, which is computed as the weighted mean of selected individuals:

$$\langle x \rangle_w^{(g)} = \sum_{i=1}^{\mu} w_i x_{i:\lambda}^{(g)}, \tag{18}$$

with $w_i > 0, \forall i = 1, \ldots, \mu$, and $\sum_{i=1}^{\mu} w_i = 1$. The indexing $i : \lambda$ is used to denote the ith best individual.

The mutation parameters, i.e. the step size $\sigma^{(g)}$ and the covariance matrix $\mathbf{C}^{(g)}$, are automatically tuned by the algorithm. Such procedure happens in two steps. First of all, the global step size undergoes an adaptation process. Afterwards, $\mathbf{C}^{(g)}$ is updated according to the evolution path, the μ weighted difference vectors of the newly selected parents, and the last recombination point [16].

4.1.4 Combining EGO and CMA-ES in the HKG-LSM

The main contribution of this paper is to exploit the complementarity of CMA-ES and EGO to increase the overall efficiency of the global optimization of computationally expensive functions [26]. This is motivated by the insight that EGO constructs

approximations of high-fidelity models using the values of the expensive objective function at chosen training samples and improving the surrogate by adding new points to this low-fidelity model. In contrast to this, CMA-ES samples new points according to a multivariate normal distribution to converge towards the optimum by means of recombination and mutation. As a consequence, it seems to be natural to take advantage of the different potentials that both methods exhibit at different stages of the optimization process. This leads to an algorithm that (i) starts with a DoE characteristic for surrogate-based optimization techniques and fitting an initial Kriging approximation of the high-fidelity model. Then, (ii) it continues with the optimization of the Kriging model using the adaptive infill procedures from EGO. In the next step, (iii) it switches to CMA-ES for final refining and convergence as soon as no further improvement on the objective function value is observed for a prescribed number of iterations. The total approach proposed in this work is referred here as Hybrid Kriging-assisted Level Set Method for Structural Topology Optimization. It may be also used outside of the context of topology optimization, e.g. for shape, size and material optimizations. To realize the sequential coupling proposed by HKG-LSM, a predefined constant value, $c_{\max}$, is compared to c, which is the counter of iterations without any improvement of the optimum. If EGO finds a better design before the value $c_{\max}$ is reached, i.e. for $c \leq c_{\max}$, the first sub-algorithm is continued and the counter is reset to zero. Otherwise the CMA-ES is started. The $c_{\max}$ parameter can be chosen according to the considered problem, but, as discussed later in this work, it is convenient that the transition to CMA-ES occurs once the explorative capabilities of KG-LSM are sufficiently exploited.

At the moment of the switch between the considered sub-algorithms, the mutation step size σ of the CMA-ES optimizer is taken as the exponentially weighted average (EWA) of the differences in position between the unpromising infill points, i.e. worse than the current best, and the current best design during the last $c_{\max}$ iterations of the KG-LSM, rescaled by a constant scalar α. Such EWA is iteratively computed over the $c \leq c_{\max}$ iterations as follows:

$$v_c = \begin{cases} x_{i,1}, & \text{if } c = 1 \\ \beta v_{c-1} + (1-\beta) x_{i,c}, & \text{if } c > 1 \end{cases} \tag{19}$$

where the coefficient β represents the degree of weighting decrease, a constant smoothing factor between 0 and 1 and chosen in this work equal to 0.1 (a lower β discounts newer observations faster), $x_{i,c}$ is the value of the ith component of the infill design at a time period c, and v_c is the value of the EWA at any iteration, c. Equation (19) applies weighted factors to the positions of the infill points so that the most recent candidates have greater influence on the stepsize definition. This choice for the σ parameter is aimed to take into account the predominant tendency of the KG-LSM to explore/exploit the design space during the unsuccessful search of a new current optimum within the prescribed number of iterations $c_{\max}$, leading to a larger/stricter mutation step size for the ES as soon as the transition occurs.

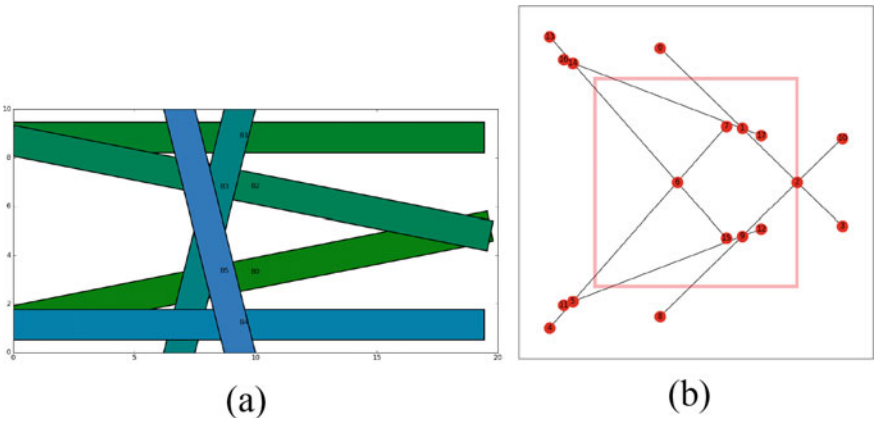


Fig. 4 One-to-one correspondence between the beam structure and its graph representation [33]

4.2 Constraint Handling Techniques

During the DoE phase of the optimization algorithm, the infeasible sample points are automatically discarded and only the feasible ones are used to construct the surrogate approximation. On the other hand, different techniques are used to deal with the connectivity and volume constraint during the infill procedure.

4.2.1 Expected Improvement for Connected Designs

The Expected Improvement for Connected Designs (EICD) is a variant of the standard EI, defined to ensure the connectivity of the promising candidates during the infill procedure [32, 33]. The main idea is to penalize the disconnected designs according to the level of infeasibility. By means of a mapping to a two-dimensional graph representation (Fig. 4), when disconnected designs are met during the maximization of EI by Differential Evolution (DE) [36], the algorithm computes a penalty P, which takes into account the amount of violation of the connectivity constraint:

$$P = \gamma(P_1 + P_2 + P_3), \tag{20}$$

where each P_i, for $i = 1, 2, 3$, is the minimum extra-distance that has been computed according to the 1st, 2nd or 3rd type of disconnection presented in Sect. 3, and γ is a suitable penalty factor.

Such penalty is used to modify the EI criterion in Eq. (16) as follows:

$$\text{EICD}(\mathbf{x}) = \begin{cases} E[I(\mathbf{x})] & \text{if } \mathbf{x} \text{ is connected,} \\ -P(\mathbf{x}) & \text{if } \mathbf{x} \text{ is disconnected.} \end{cases} \tag{21}$$

Here, the introduction of the penalty P is dictated by the necessity to avoid the creation of large flat areas in the landscape of the optimization problem, which might cause stagnation of the DE search. As a result, the designs infeasible according to the connectivity constraint are automatically discarded in the maximization of Eq. (21). Therefore, since the convergence speed is measured in terms of evaluations, the proposed strategy does not evaluate the objective function on disconnected designs and hence it speeds up the convergence towards the optimum.

4.2.2 Constrained Expected Improvement

In this study, the Constrained Expected Improvement (CEI) [13] is used to generate points that satisfy a prescribed volume limit. At each iteration of the optimization strategy, when the Kriging surrogate is fitted on the previous training set and the EI function is computed, an approximation of the function defining the volume constraint is also constructed. Let $Y(\mathbf{x}) = N(\hat{y}(\mathbf{x}), \hat{s}^2(\mathbf{x}))$ be the Kriging model for the objective function. Then, the surrogate model for the constraint is:

$$G(\mathbf{x}) = N(\hat{g}(\mathbf{x}), \hat{\sigma}^2(\mathbf{x})), \tag{22}$$

where $\hat{g}(\mathbf{x})$ is the prediction of the constraint function and $\hat{\sigma}^2(\mathbf{x})$ is the variance of the model of the constraint. At this stage, the probability that the design satisfies the volume constraint (Probability of Feasibility (PF)) is computed as:

$$P[F(\mathbf{x})] = \frac{1}{\hat{\sigma}^2(\mathbf{x})\sqrt{2\pi}} \int_0^\infty \exp\left(-\frac{(F - \hat{g}(\mathbf{x}))^2}{2\hat{\sigma}^2(\mathbf{x})}\right) dG, \tag{23}$$

where $\hat{g}(\mathbf{x})$ is the prediction of the constraint function, $\hat{\sigma}^2(\mathbf{x})$ is the variance of the model of the constraint, and $F = G(\mathbf{x}) - V_{\text{req}}$ is the entity of feasibility. Hence, the probability that a feasible infill point improves on the best value so far can be computed by maximizing the product between EI and PF:

$$\mathbf{x}_{\text{infill}} = \underset{\mathbf{x}}{\text{argmax}} \ \text{CEI}(\mathbf{x}) = \underset{\mathbf{x}}{\text{argmax}} \ E[I(\mathbf{x})]P[F(\mathbf{x})], \tag{24}$$

where the product is justified by the independence of the models.

In order to consider both the connectivity and volume constraints, the coupling between EICD and CEI is obtained by applying the connectivity check in the maximization of EI·PF, leading to the following combined definition:

$$\overline{\text{EICD}}(\mathbf{x}) = \begin{cases} \text{CEI}(\mathbf{x}) & \text{if } \mathbf{x} \text{ is connected,} \\ -P(\mathbf{x}) & \text{if } \mathbf{x} \text{ is disconnected.} \end{cases} \tag{25}$$

4.2.3 Exterior Penalty Method

The preceding techniques are appropriate for the Kriging-based EGO. Therefore, in the second part of the optimization process, when CMA-ES comes in, another method to handle the constraints has to be introduced: the Exterior Penalty Method [31], which is commonly used by optimization strategies involving Evolutionary Algorithms. The mechanism of penalty functions is the most uniformly applicable approach to deal with constrained design. It works by penalizing the objective function values every time a constraint is not satisfied. Therefore, the objective function assumes the following shape:

$$f(\mathbf{x}) = f_{\text{obj}}(\mathbf{x}) + \gamma \cdot \max(0, g(\mathbf{x})), \tag{26}$$

where f_{obj} is the objective function to be minimized in the original problem, g is a nonlinear constraint and γ denotes a penalty constant. This leads to a modification of the objective function value that automatically rejects the penalized design. The penalty is usually taken as a very large constant value, in order to immediately ensure rejection of an infeasible design. The penalized objective function is referred to as *cost function*. When using surrogate approximations, adding such a big value is not the best approach to avoid infeasible designs. In fact, it would lead to severe discontinuities in the shape of the penalized fitness function and such modifications would artificially and severely influence the surrogate approximation.

5 Test Case

Firstly, the proposed HKG-LSM optimization strategy is evaluated on a linear elastic test case at two different dimensionalities, which is characterized by low computational costs and is already sufficient to draw some conclusions about the promisingness of the approach. The test is performed on the standard cantilever beam benchmark problem, whose structure is optimized to minimize compliance. Afterwards, the algorithm is applied to a dynamic transverse bending test case, for which standard topology optimization techniques are not suitable. The previously developed KG-LSM [32, 33] and the EA-LSM, using CMA-ES [7, 17], are taken as a reference to compare the convergence properties and the optimized designs resulting from the proposed approach.

5.1 Linear Elastic Case

The first case study is the standard cantilever beam benchmark test case, whose structure is optimized to minimize compliance. As shown in Fig. 5a, the beam is fixed to a support at the left-hand side and a static unit load is applied in the middle

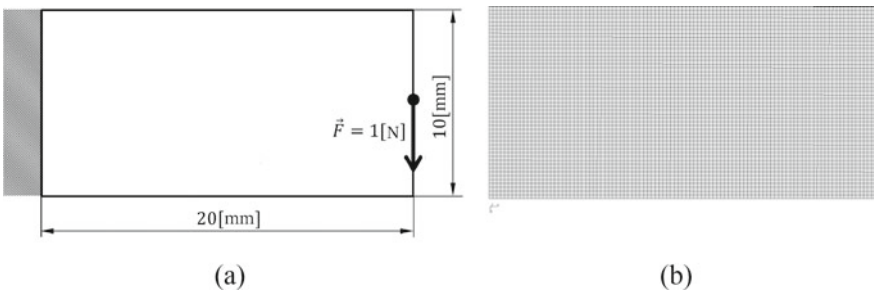


Fig. 5 Cantilever beam test case: **a** problem definition and **b** CalculiX FEM mesh [33]

Table 1 Cantilever beam test case settings

Property	Symbol	Value	Unit
Beam mass density	ρ	$7,85 \cdot 10^3$	kg/m^3
Young's modulus	E	$2.1 \cdot 10^5$	MPa
Poisson's ratio	ν	0.3	–
Load	F	1	N
Required volume fraction	V_f	50%	–
Mesh resolution	–	100 x 50	–
Element type	–	Four-node shell element	–
Solver	–	CalculiX 2.9	–

of the right-hand side. The domain dimensions are 20×10 [mm]. The LSF is here mapped to a CalculiX[1] FEM mesh (Fig. 5b), where a very low density space (1% of the material density) is assigned to the areas occupied by void. The domain dimensions are 20×10[mm] and it is discretized with 5000 four-node square shell (S4R) finite elements, arranged in a 100×50 grid. The test settings are shown in Table 1.

In order to validate the presented method, the 6-beams diagonal layout of beams depicted in Fig. 6 is used. This layout is used to evaluate the method in a 9-variables environment first [34], where both the x and y coordinates of the beams' barycenter, as well as their orientation, are free to vary during the optimization, and in a 15-variables test afterwards, where all the parameters defining the local LSFs are allowed to change. A symmetry of the design with respect to the domain horizontal symmetry axis is assumed throughout the optimization process.

[1]CalculiX is an open-source, 3D structural FEM software developed at MTU Aero Engines in Munich. CalculiX, Version 2.13, was used in this work: http://www.calculix.de/.

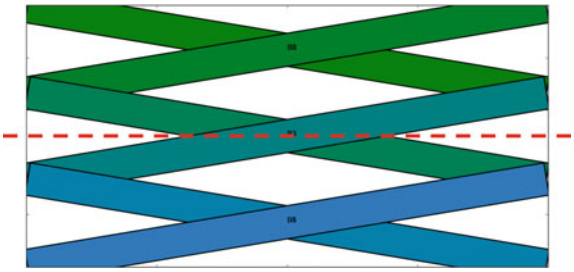


Fig. 6 Reference layout of 6-beams for the static cantilever beam test case [33]

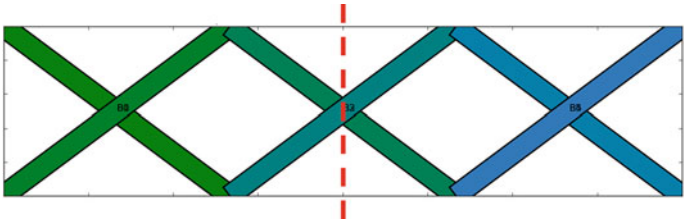


Fig. 7 Initial reference 6-beams configuration for the dynamic transverse bending test case [33]

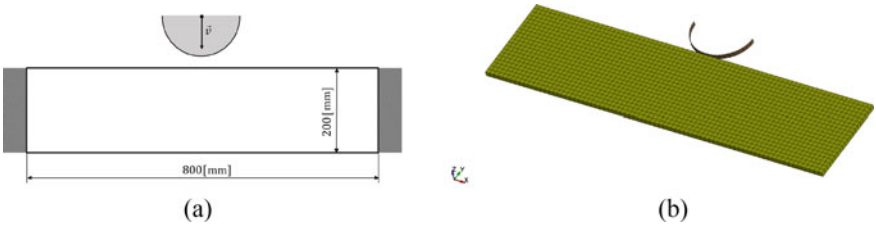


Fig. 8 Transverse bending test case: **a** problem definition and **b** LS-Dyna FEM mesh [33]

5.2 Nonlinear Crash Case

The final aim of this study is to propose an algorithm performing well in the continuous global optimization of expensive and multimodal problems, e.g. associated with vehicle crashworthiness. In this work, the proposed application to a crashworthiness optimization problem consists of a 6-beams and 15-variables transverse bending test case (Fig. 8), starting from the reference layout shown in Fig. 7. As for the 15-variables static test case, during the optimization process, all the parameters characterizing the moving morphable components are allowed to vary. However, in this case a symmetry condition with respect to the domain vertical symmetry axis is imposed.

More precisely, the crash experiments involved a pole impact on a beam supported at both ends, as illustrated in Fig. 8a. The optimization task is to minimize the dynamic

Table 2 Configuration of the transverse bending test case

Property	Symbol	Value	Unit
Beam mass density	ρ	$2.7 \cdot 10^3$	kg/m^3
Young's modulus	E	$7.0 \cdot 10^4$	MPa
Poisson's ratio	ν	0.33	–
Yield strength	R_e	241.0	MPa
Tangent modulus	E_{tan}	70.0	MPa
Initial pole velocity	v	20	m/s
Pole mass	m	11.815	kg
Pole diameter	D	139.154	mm
LS-Dyna termination time	t_{end}	1.5	ms
LS-Dyna mesh resolution	–	80×20	–
Solver	–	LS-DYNA R7.1.1	–
Element type	–	Eight-node solid element	–

intrusion of the impactor into the structure, i.e., the intrusion preceding the elastic rebound. The LSF function is mapped on a reference LS-Dyna mesh, as illustrated in Fig. 8b. It is composed of 1600 eight-node solid elements with a piecewise linear plasticity material and fixed in the z direction throughout the optimization procedure. In particular, an elasto-plastic material defined by an isotropic von Mises plasticity model with linear hardening is used [23, 24]. In order to assure a physically correct crash behavior, the elements in the areas occupied by void are deleted from the mesh. The properties of the material are shown in Table 2.

6 Experimental Setup

This section describes the experimental setup used to test the proposed HKG-LSM and the obtained results. Since this study aims to extend the experimental evaluation presented by Raponi et al. [34], where the HKG-LSM is tested on a 6-beams 9-variables configuration under static loading conditions, here the same algorithm is validated on a 15-variables configuration in both a static and dynamic test case.

The following strategies are compared for a total budget of 500 calls to the objective function:

– HKG-LSM-bias(n)-exp: Hybrid Kriging-guided Level Set Method where the switch from KG-LSM to CMA-ES is done when the best observed objective value is not updated for n iterations; the step size for CMA-ES is chosen as the exponen-

tially weighted average of the distances between the best structure and the worse infill points;
- KG-LSM: Kriging-guided optimization method with initial DoE selection by removing the infeasible points and the $\overline{\text{EICD}}$ to handle both the connectivity and the volume constraint during the infill procedure. It is shown for comparison purposes;
- EA-LSM using CMA-ES and taking the reference structure in Fig. 6 as first parent design. Here, the exterior penalty method is used to drive the search towards feasible designs. It is shown for comparison purposes.

In the 9-variables static test case, the surrogate-based algorithms start from a 300-samples DoE. Three versions of the hybrid method are analyzed, which differ in the chosen bias n ($n = 10, 30, 50$) guiding the switch between the sub-algorithms. In the KG-LSM optimization algorithm, $\theta_L = [1\text{E-}3] * 9$ and $\theta_U = [1\text{E}3] * 9$ are chosen as user-defined bounds for the theta parameter to be optimized through Maximum Likelihood Estimation, as explained in Sect. 4.1.1. They characterize the correlations between the approximation variables, which are chosen as squared-exponential functions. A non-elitist (μ, λ)-CMA-ES strategy is used and initialized with a parent population of $\mu = 5$ individuals, whereas $\lambda = 10$ is the offspring population size. This means that the best individuals are reselected at each iteration of the algorithm through a recombination plus mutation procedure. The mutation step is characterized by a normally distributed random vector defined by the initial mean m_{init}, while the standard deviation σ_{init} is chosen in this work as the exponentially weighted average described in Sect. 4.1.4.

The static and dynamic 15-variables test cases are compared for the same budget of 500 evaluations of the objective function, starting from a 600-samples and 200-samples DoE, respectively. This choice was dictated by the fact that in the crash test case it is much easier to obtain feasible structures according to the connectivity constraint rather than in the static one, which requires the connection of the structural layout to the point where the load is applied on the right-hand side of the domain. In both cases, the same three algorithms are compared, with the only difference that HKG-LSM is tested with a switch bias fixed to 50 and 100. By analogy with the 9-variables test case, in the KG-LSM optimization algorithm $\theta_L = [1\text{E-}3] * 15$ and $\theta_U = [1\text{E}3] * 15$ are chosen as bounds for the theta parameter to be optimized through Maximum Likelihood Estimation, and non-elitist (6, 12)-CMA-ES strategy is used.

7 Results

In this section, the results obtained for each of the described test cases are shown. HKG-LSM is compared with the state-of-the-art CMA-ES and the novel KG-LSM in a constrained static environment for two different problem dimensionalities (Sects. 7.1 and 7.2), as well as in a crash scenario (Sect. 7.2). Due to the non-

deterministic nature of the considered optimization algorithms, for each one 30 optimization runs are performed (with different random seeds).

7.1 9-Variables Linear Elastic Case

The comparison is first drawn on the static cantilever beam benchmark test case in a 9-variables [34] and in a 15-variables test case. The results obtained in each case are shown below.

For each strategy, the average convergence of the compliance objective function in terms of evaluations is shown in Fig. 9. Here, the objective function is normalized with respect to the reference design for the 6-beams test case defined in Sect. 5.1. Figure 9 shows that when evaluation 280 is reached, CMA-ES seems more suitable for exploiting the best design obtained so far, leading to a better performance over KG-LSM. When observing the HKG-LSM strategies, the predominance of CMA-ES is not evident anymore. In fact, the hybrid techniques take advantage of the initial rapid decrease of the objective function resulting from the Kriging-based optimization and, when no improvement is detected within a certain number of iterations, the algorithm transits to CMA-ES. The HKG-LSM-bias50-exp provides a better convergence trend than the other hybrid techniques. Indeed, an early switch to the CMA-ES might cause an excessive exploitation of a partially optimized design, increasing its probability to converge to a local optimum. On the other hand, a late transition from KG-LSM to CMA-ES has a better chance of bringing to the ES a design that is the result of a more explorative strategy, which did not focus on localized areas of the problem domain, but rather found optimal designs by searching emptier areas, characterized by a high variance of the surrogate model. Such considerations can be validated by the following analysis. According to Fig. 10, three main groups of material distributions, each representing a different (local) optimum obtained by the HKG-LSM-bias50-exp, can be distinguished. The frequency with which they have been observed are the 20%, 20%, and 40%, for the first, second and third optimum respectively. On the other hand, the same local optima could be detected after the inspection of the results obtained for the HKG-LSM-bias10-exp. Here, the percentages drop to 7%, 7%, and 53%, respectively. Such data demonstrate that a premature switch to the CMA-ES might give preference to local optima, leading to a worse convergence trend for the minimization of the cost function.

In general, from the final structures optimized by HKG-LSM (Fig. 10), it can be deducted that such methods allow sufficient flexibility for reaching designs that are not far from the theoretical one presented by Michell [25] for a 6-beams configuration, showed in Fig. 11. In fact, at this stage, the quality of the obtained beam configurations is affected by the impossibility to vary the length and thickness parameters of the beams. To conclude, further information about the optimized cost values can be found in Fig. 12, which presents the statistics for each method after 100, 250 and 500 evaluations. In order to compare the medians reached by the different optimization strategies, the statistical Wilcoxon rank sum test is used. At evaluation

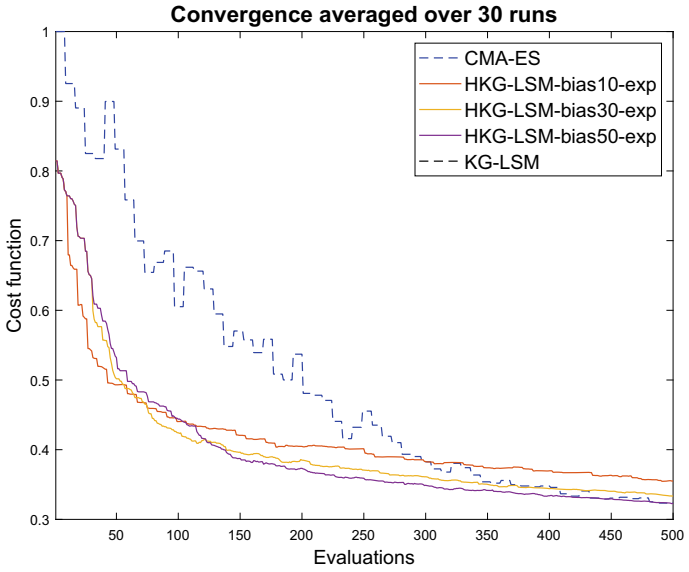


Fig. 9 Convergence of the compliance function averaged over 30 runs for the 9-variables linear elastic test case. HKG-LSM starts from a 300-samples DoE, with selection of feasible designs. The trends for the 10, 30 and 50-iterations bias for the switch are compared. The evaluations spent for the DoE phase are not shown in the plot since they are performed once for all the methods. The KG-LSM and the CMA-ES are also shown as a reference [34]

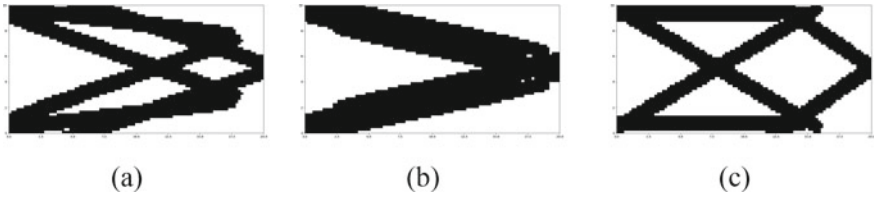


Fig. 10 Three main topology types obtained with the HKG-LSM-bias50-exp method and the frequency with which they have been developed in 30 optimization runs. **a** First optimum: 20%. **b** Second optimum: 20%. **c** Third optimum: 40% [34]

500, the null hypothesis that data from the different optimization methods have equal medians at the 5% significance level is not rejected when comparing HKG-LSM-bias30/50-exp with CMA-ES. This means that these strategies are comparable at the end of the considered maximum range of evaluations. Moreover, if evaluating the statistics at the beginning of the optimization process (after 100 evaluations), the same null hypothesis is rejected when comparing CMA-ES with the HKG-LSM strategies. Therefore, the HKG-LSM converges much faster than CMA-ES towards the optimum, validating the promisingness of surrogate-based strategies in case if a strict budget of evaluations is imposed.

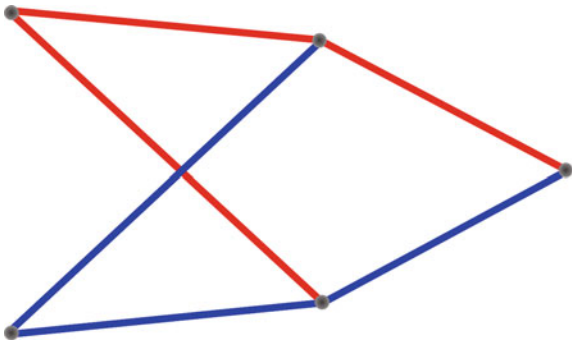


Fig. 11 Michell theoretical model for a 6-beams static test case [34]

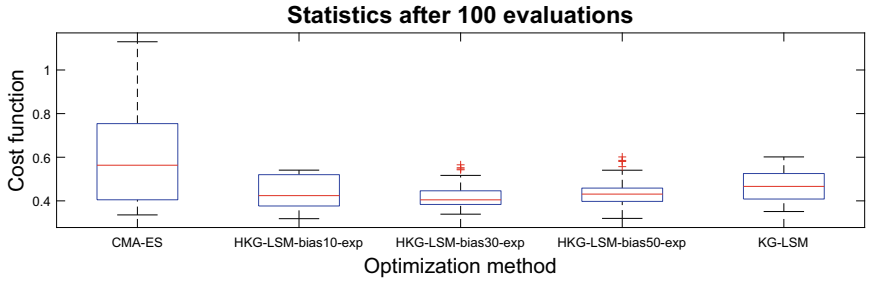
7.2 15-Variables Test Cases

Since this work is an extension of the study presented by Raponi et al. [34] on a static 9-variables test case, more experiments were carried out at a higher dimensionality in both, a static and a dynamic environment, where the optimal layout is obtained by allowing the six MMCs to vary in x-position and y-position of the barycenter, orientation, length and thickness, and it is hence defined by a vector of 15 parameters due to the symmetry condition. These scenarios are described below.

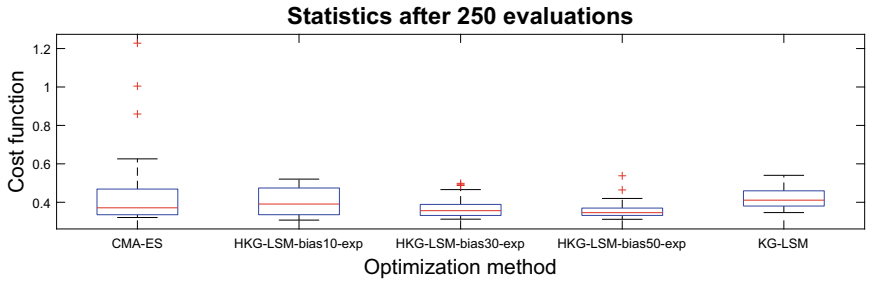
7.2.1 Linear Elastic Case

Although the dimensionality of the problem is increased, the same 6-beams configuration of the 9-variables test case (Fig. 6) is also used as reference design for the 15-variables static test case. For each compared optimization strategy, the average compliance over the 30 runs in terms of evaluations is shown in Fig. 13, where the objective function is normalized with respect to the compliance measured for the design in Fig. 6. By taking advantage of previous knowledge, the hybrid technique is tested in two variants, allowing the switch from KG-LSM to EA-LSM when no improvement on the best recorded value is obtained for 50 or 100 consecutive evaluations. Moreover, the convergence trends of the surrogate-based strategies start from an average value resulting from an initial DoE of 600 samples, where only the connected designs are selected and evaluated, while the infeasible ones are automatically discarded.

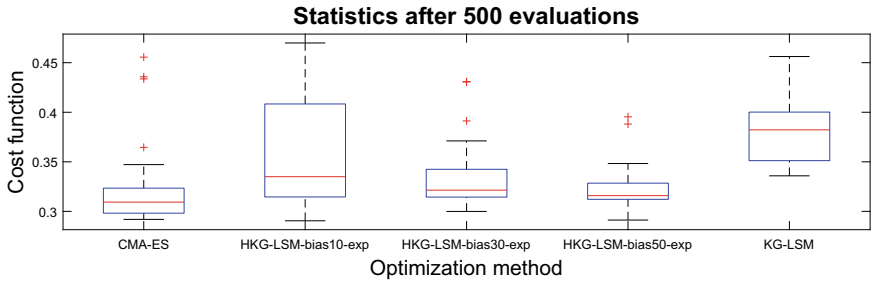
From Fig. 13 it can be observed that, even if the dimensionality of the problem is increased, the hybrid strategies outperform KG-LSM and are preferable to CMA-ES within the prescribed budget of evaluations. In fact, while KG-LSM shows a better performance than CMA-ES until evaluation 200, HKG-LSM-bias50-exp and HKG-LSM-bias100-exp are characterized by a faster convergence at the beginning of the optimization process and comparable cost function values just at the end. A further remark to the convergence trends is about the different behavior shown by



(a)



(b)



(c)

Fig. 12 Statistical evaluation of the optimization methods compared for the 6-beams 9-variables cantilever beam test case: box plots for 30 runs after **a** 100, **b** 250, and **c** 500 evaluations [34]

the hybrid strategies with respect to the previous test case. While in the 9-variables static test case, a postponed switch leads to an overall better convergence towards the optimum, in the the 15-variables static test case, the switch after 100 evaluations with no improvement on the optimal layout is not preferable to the one after 50 evaluations. This might be due to a less explorative behavior of the KG-LSM algorithm, which does not produce significant updates in many of the 30 runs since the beginning of the process. In this way, many runs are stuck in the same local regions regardless of

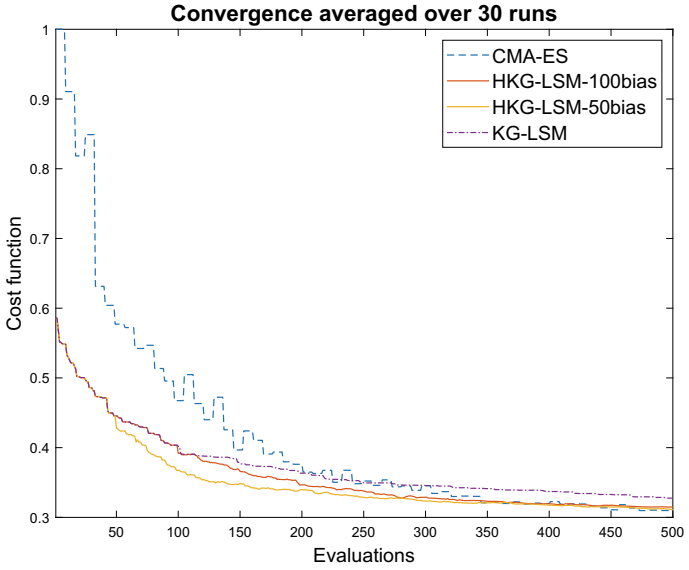


Fig. 13 Convergence of the compliance function averaged over 30 runs for the 15-variables linear elastic test case. HKG-LSM starts from a 600-samples DoE, with selection of feasible designs. The trends for a 50 and 100-iterations bias for the switch are compared. The KG-LSM and the CMA-ES trends are also shown as a reference

the moment when the switch between KG-LSM and EA-LSM occurs, and hence do not benefit from a delayed switch.

Further information about the optimized cost values can be found in Fig. 16a, which presents the statistics for each method after 100, 250 and 500 evaluations. Again, the statistical Wilcoxon rank sum test is used. At evaluation 500, the null hypothesis that data from the different optimization methods have equal medians at the 5% significance level is accepted when comparing HKG-LSM-bias50/100-exp with CMA-ES, while it is rejected in the comparison of the hybrid strategy with KG-LSM. At evaluation 100 and 250, the same null hypothesis is rejected when comparing HKG-LSM-bias50-exp with all the other strategies. This implies that HKG-LSM is statistically significantly better than KG-LSM, while allows for a faster convergence towards an optimum if compared to CMA-ES.

Finally, although the layouts resulting from each of the compared optimization strategies are not satisfactory (pointing out the need for a wider budget of evaluations in higher-dimensional problems), at evaluation 500 almost all the designs reached by CMA-ES can be classified into three main groups of material distributions, as illustrated in Fig. 14. The frequency with which they have been observed are the 13%, 30%, and 47%, for the first, second and third optimum respectively, amounting in total to the 90% of all the designs. On the other hand, the same local optima could be detected after the inspection of the results obtained for the HKG-LSM-bias50-exp with percentages dropping only to the 7%, 27% and 17%, respectively, while the

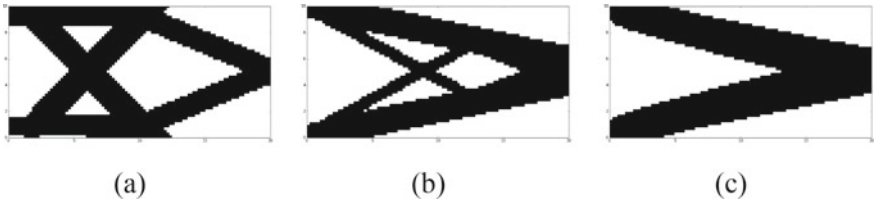


Fig. 14 Three main topology types obtained with the CMA-ES method and the frequency with which they have been developed in 30 optimization runs. **a** First optimum: 13%. **b** Second optimum: 30%. **c** Third optimum: 47%

other designs cannot be classified into categories. From these data it can be observed that while CMA-ES is able to reach clearly defined local optima when used as single algorithm, it is has reduced explorative capabilities when used as sub-algorithm in the hybrid strategies. As a consequence, taking advantage of the KG-LSM exploration as much as possible at the beginning is of the utmost importance. Therefore, an optimization study on the number of evaluations preceding the switch needs to be done.

7.2.2 Nonlinear Crash Case

A 6-beams 15-variables problem is introduced in this work to evaluate the HKG-LSM capabilities in a constrained crashworthiness environment. The same optimization strategies compared in the 15-variables static test case are here analyzed. For each strategy, the average convergence of the compliance objective function in terms of evaluations is shown in Fig. 15. In analogy with the static case, the objective function is normalized with respect to the reference design for the 6-beams test case defined in Sect. 5.2. The convergence trends of the surrogate-based strategies start from an average value resulting from an initial DoE of 200 samples, with selection of feasible designs. From Fig. 15, it is worth noting that, due to its ability to balance exploration and exploitation, KG-LSM already outperforms CMA-ES within the whole budget of available evaluations. However, it still makes sense to test the hybridization procedure due to the different convergence curves produced by the surrogate-based and the evolution strategy. Indeed, while KG-LSM makes early progress and then loses efficiency, CMA-ES steadily converges to the minimum as the number of calls to the objective function increases. Therefore, a switch to the second strategy can be beneficial in view of a final tuning of an optimal configuration of beams. However, such improvement on the KG-LSM performance was not observed in the studied test case.

On the other hand, if looking at the box plots in Fig. 16b and by the results from the statistical testing, it can be assessed that HKG-LSM is statistically significantly better than CMA-ES and comparable to KG-LSM during all the optimization procedure. Therefore, in this crash scenario where the previously introduced KG-LSM already

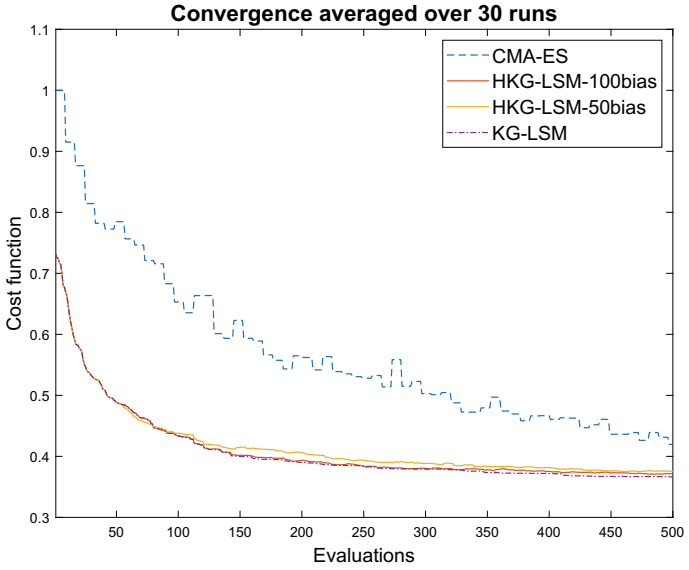


Fig. 15 Convergence of the intrusion function averaged over 30 runs for the nonlinear crash test case. HKG-LSM starts from a 200-samples DoE, with selection of feasible designs. The trends for a 50 and 100-iterations bias for the switch are compared. The KG-LSM and the CMA-ES trends are also shown as a reference

performs satisfactorily, the hybrid strategy does not worsen the optimization outcome from the statistical point of view. To the authors' opinion, HKG-LSM would be much more efficient in case if a even higher dimensional test case is considered, where a pure surrogate-based strategy would exhibit some deficiencies.

Finally, similar topology types are obtained by all the surrogate-based strategies, demonstrating that HKG-LSM can be efficiently used at the early stages of the design process of mechanical structures targeted to face dynamic loads. The main topologies and the frequencies with which they have been observed are shown in Table 3.

8 Conclusions

This study is an extension of the work by Raponi et al. [34]. The main aim was to evaluate the potential of the Hybrid Kriging-assisted Level-Set Method (HKG-LSM) for Topology Optimization (TO) in higher-dimensional test cases and under dynamic loading conditions. The whole research is motivated by the need for cheap procedures in modern automotive industry, where optimization strategies demonstrated to be good alternatives to the classical trial and error method. Aimed to final applications to the crashworthiness design optimization field, where no gradient information is available, Efficient Global Optimization (EGO) with the use of Surrogate Models -

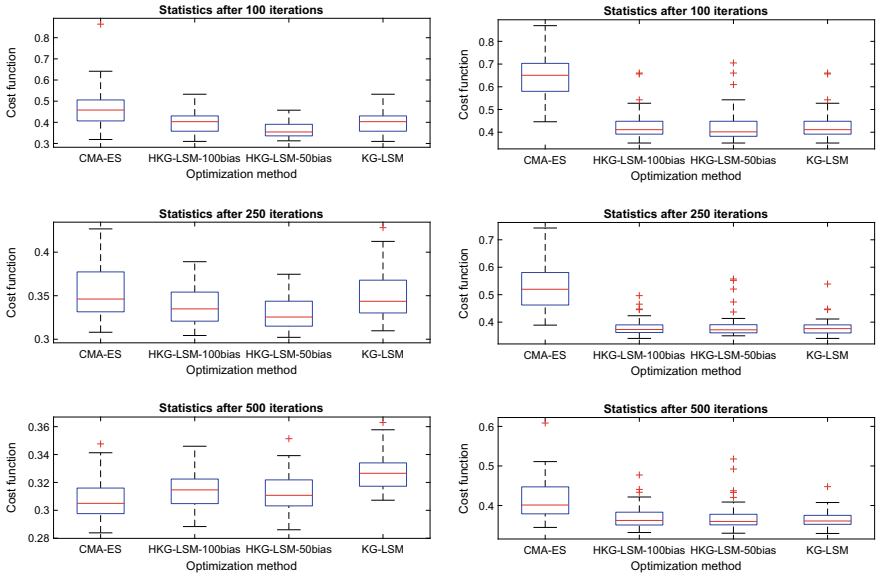


Fig. 16 Statistical evaluation of the optimization methods compared for the 15-variables cantilever beam test case **a** and the 15-variables transverse bending test case **b**. Box plots for 30 runs after 100, 250, and 500 evaluations

Table 3 Main topology types and frequencies with which they have been observed, ordered according to decreasing structural performance, for the 15-variables dynamic test case. Out of the 30 runs, the topology classification is made by visual inspection and it is based on the main characteristics determining the design (number of connections to the supports, final beam components, presence of cross sub-configurations)

Topology type	KG-LSM (%)	HKG-LSM-bias50-exp (%)	HKG-LSM-bias100-exp (%)
	23	13	20
	3	3	3
	30	30	30

Kriging in this case - and Evolution Strategies (ESs), CMA-ES in particular, represent valid alternatives. Their principles are different, yet complementary: EGO constructs an approximation of the high-fidelity model by evaluating the expensive objective function on a chosen training set and improves the optimum by adding new points to the model, while CMA-ES learns and samples multi-normal laws in the space of designs variables and converges towards the optimum by means of a recombination and mutation process of the individuals. Such algorithms are used by the Kriging-guided Level Set Method (KG-LSM) and the Evolutionary Level Set Method (EA-LSM) for structural TO, which are the two sub-algorithms composing the HKG-LSM optimization strategy. Starting with an initial set of training points generated by the Design of Experiments (DoE) and thanks to the surrogate-based technique, a fast convergence of the objective function towards the optimum is obtained at the beginning of the optimization process. Afterwards, CMA-ES is used to exploit some promising areas of the domain, leading to a refined design with a competitive fitness if compared to its neighbors.

In this research, the potential of the proposed HKG-LSM was first assessed through the study of a standard cantilever beam benchmark test case in optimization problems of different dimensionalities (up to 15 variables), where the objective function to be minimized was the compliance of the structure. Afterwards, an application to a dynamic transverse bending test case with intrusion minimization was presented to show the suitability of the method in a crashworthiness application.

In the static test cases, HKG-LSM led to significant improvements of the convergence properties in the initial stages of the optimization process, if compared to KG-LSM and EA-LSM. When coming to the dynamic test case, the considered application was characterized by an already good performance of the novel KG-LSM, if compared to EA-LSM. No improvement on the convergence trend could be hence observed for the hybrid strategy. However, HKG-LSM turned out to be superior to EA-LSM and comparable to KG-LSM both in terms of convergence speed and generated optimal layouts. Therefore, the proposed approach can be in general a valid alternative to both the surrogate-based and evolutionary-based methods, if taken alone, in the optimization of mechanical structures. Indeed, it was characterized by a fast convergence at the beginning of the optimization process in each of the considered test cases. Since HKG-LSM is finalized to crashworthiness optimization problems, which are characterized by a limited number of available evaluations, the proposed hybrid technique is promising. Consequently, further studies on test cases of higher dimensionality are planned to be done in future works. To this end one option is to couple the Clement method with the novel PCA-Bo [35]. Moreover, a procedure to optimize the number of evaluations preceding the switch and some deeper analysis with regards to the estimation of the initial parameters for the CMA-ES are needed. In fact, the fitted Kriging mean as an approximation to the true function can be used to initialize both the covariance matrix and the step size of CMA-ES [26]. Lastly, new methods to combine surrogates with evolution strategies in order to obtain outperforming mechanical structures can be investigated.

References

1. Allaire, G., Jouve, F., Toader, A.M.: Structural optimization using sensitivity analysis and a level-set method. J. Comput. Phys. **194**(1), 363–393 (2004). https://doi.org/10.1016/j.jcp.2003.09.032
2. Arsenyev, I.: Efficient Surrogate-based Robust Design Optimization Method. Ph.D. thesis, Technische Universität München (2017)
3. Aulig, N.: Generic topology optimization based on local state features. Ph.D. thesis, Technische Universität Darmstadt, VDI Verlag, Germany (2017)
4. Aulig, N., Olhofer, M.: State-based representation for structural topology optimization and application to crashworthiness. In: 2016 IEEE Congress on Evolutionary Computation (CEC), Vancouver, Canada, pp. 1642–1649 (2016). https://doi.org/10.1109/CEC.2016.7743985
5. Bendsøe, M.P., Sigmund, O.: Topology Optimization - Theory, Methods, and Applications, 2nd edn. Springer, Berlin (2004). http://www.springer.com/cn/book/9783540429920
6. Bujny, M., Aulig, N., Olhofer, M., Duddeck, F.: Evolutionary level set method for crashworthiness topology optimization. In: VII European Congress on Computational Methods in Applied Sciences and Engineering, Crete Island, Greece (2016)
7. Bujny, M., Aulig, N., Olhofer, M., Duddeck, F.: Identification of optimal topologies for crashworthiness with the evolutionary level set method. Int. J. Crashworthiness **23**(4), 395–416 (2018). https://doi.org/10.1080/13588265.2017.1331493
8. Cressie, N.: The origins of kriging. Math. Geol. **22**(3), 239–252 (1990). https://doi.org/10.1007/BF00889887
9. Duddeck, F., Volz, K.: A new topology optimization approach for crashworthiness of passenger vehicles based on physically defined equivalent static loads. In: ICrash International Crashworthiness Conference, Milano, Italy (2012)
10. Duddeck, F., Hunkeler, S., Lozano, P., Wehrle, E., Zeng, D.: Topology optimization for crashworthiness of thin-walled structures under axial impact using hybrid cellular automata. Struct. Multidiscip. Optim. **54**(3), 415–428 (2016). https://doi.org/10.1007/s00158-016-1445-y
11. Eschenauer, H.A., Kobelev, V.V., Schumacher, A.: Bubble method for topology and shape optimization of structures. Struct. Optim. **8**(1), 42–51 (1994). https://doi.org/10.1007/BF01742933
12. Fang, K.T., Li, R., Sudjianto, A.: Design and Modeling for Computer Experiments. CRC Press (2005)
13. Forrester, A.I.J., Sóbester, A., Keane, A.J.: Engineering Design via Surrogate Modelling - A Practical Guide. John Wiley & Sons Ltd. (2008)
14. Guo, X., Zhang, W., Zhong, W.: Doing topology optimization explicitly and geometrically - a new moving morphable components based framework. J. Appl. Mech. **81**(8), 081009 (2014). https://doi.org/10.1115/1.4027609
15. Haber, R., Bendsøe, M.P.: Problem formulation, solution procedures and geometric modeling: key issues in variable-topology optimization. In: 7th AIAA/USAF/NASA/ISSMO Symposium on Multidisciplinary Analysis and Optimization, St. Louis, Missouri, USA (1998)
16. Hansen, N.: The CMA evolution strategy: a tutorial (2005). https://hal.inria.fr/hal-01297037, hal-01297037f
17. Hansen, N.: The CMA evolution strategy: a comparing review. In: Towards a New Evolutionary Computation. Studies in Fuzziness and Soft Computing, pp. 75–102. Springer, Berlin (2006). https://doi.org/10.1007/3-540-32494-1_4
18. Hansen, N., Ostermeier, A.: Adapting arbitrary normal mutation distributions in evolution strategies: the covariance matrix adaptation. In: Proceedings of IEEE International Conference on Evolutionary Computation, pp. 312–317 (1996). https://doi.org/10.1109/ICEC.1996.542381
19. Hansen, N., Ostermeier, A.: Completely derandomized self-adaptation in evolution strategies. Evol. Comput. **9**(2), 159–195 (2001). https://doi.org/10.1162/106365601750190398
20. Jones, D.R., Schonlau, M., Welch, W.J.: Efficient global optimization of expensive black-box functions. J. Glob. Optim. **13**(4), 455–492 (1998). https://doi.org/10.1023/A:1008306431147

21. Kleijnen, J.P.C.: Kriging metamodeling in simulation: a review. Eur. J. Oper. Res. **192**(3), 707–716 (2009). https://doi.org/10.1016/j.ejor.2007.10.013
22. Lee, H.A., Park, G.J.: Nonlinear dynamic response topology optimization using the equivalent static loads method. Comput. Methods Appl. Mech. Eng. **283**, 956–970 (2015). https://doi.org/10.1016/j.cma.2014.10.015
23. Livermore Software Technology Corporation (LSTC), P. O. Box 712 Livermore, California 94551-0712: LS-DYNA KEYWORD USER'S MANUAL, Volume II - Material Models (2014). lS-DYNA R7.1
24. Livermore Software Technology Corporation (LSTC), P. O. Box 712 Livermore, California 94551-0712: LS-DYNA Theory Manual (2019)
25. Michell, A.G.M.: LVIII. The limits of economy of material in frame-structures. Philos. Mag. **8**(47), 589–597 (1904). https://doi.org/10.1080/14786440409463229
26. Mohammadi, H., Riche, R.L., Touboul, E.: Making EGO and CMA-ES complementary for global optimization. In: Learning and Intelligent Optimization. Lecture Notes in Computer Science, pp. 287–292. Springer, Cham (2015). https://doi.org/10.1007/978-3-319-19084-6-29
27. Mozumder, C., Renaud, J.E., Tovar, A.: Topometry optimisation for crashworthiness design using hybrid cellular automata. Int. J. Veh. Des. **60**(1–2) (2012). https://trid.trb.org/view.aspx?id=1222579
28. Ortmann, C., Schumacher, A.: Graph and heuristic based topology optimization of crash loaded structures. Struct. Multidiscip. Optim. **47**(6), 839–854 (2013). https://doi.org/10.1007/s00158-012-0872-7
29. Osher, S., Sethian, J.A.: Fronts propagating with curvature-dependent speed: algorithms based on Hamilton-Jacobi formulations. J. Comput. Phys. **79**(1), 12–49 (1988). https://doi.org/10.1016/0021-9991(88)90002-2
30. Pedersen, C.B.W.: Topology optimization design of crushed 2d-frames for desired energy absorption history. Struct. Multidiscip. Optim. **25**(5–6), 368–382 (2003). https://doi.org/10.1007/s00158-003-0282-y
31. Rao, S.S.: Engineering Optimization: Theory and Practice. Wiley (1996)
32. Raponi, E., Bujny, M., Olhofer, M., Aulig, N., Boria, S., Duddeck, F.: Kriging-guided level set method for crash topology optimization. In: 7th GACM Colloquium on Computational Mechanics for Young Scientists from Academia and Industry. Stuttgart, Germany (2017)
33. Raponi, E., Bujny, M., Olhofer, M., Aulig, N., Boria, S., Duddeck, F.: Kriging-assisted topology optimization of crash structures. Comput. Methods Appl. Mech. Eng. **348**, 730–752 (2019). https://doi.org/10.1016/j.cma.2019.02.002
34. Raponi, E., Bujny, M., Olhofer, M., Boria, S., Duddeck, F.: Hybrid kriging-assisted level set method for structural topology optimization. In: Proceedings of the 11th International Joint Conference on Computational Intelligence (IJCCI 2019), Vienna, Austria, pp. 70–81 (2019). https://doi.org/10.5220/0008067800700081
35. Raponi, E., Wang, H., Bujny, M., Boria, S., Doerr, C.: High dimensional Bayesian optimization assisted by principal component analysis. In: Parallel Problem Solving from Nature, PPSN XVI, pp. 169–183. Springer, Cham (2020). https://doi.org/10.1007/978-3-030-58112-1_12
36. Storn, R., Price, K.: Differential evolution a simple and efficient heuristic for global optimization over continuous spaces. J. Glob. Optim. **11**(4), 341–359 (1997). https://doi.org/10.1023/A:1008202821328